




RESEARCH ARTICLE

The Insulin Receptor and Insulin like Growth Factor Receptor 5' UTRs Support Translation Initiation Independently of EIF4G1

Nicholas K. Clark,^{a,b} Meghan T. Harris,^{a,c} William B. Dahl,^a Zachary Knotts,^a  Michael T. Marr II^a

^aDepartment of Biology and Rosenstiel Basic Medical Sciences Research Center, Brandeis University, Waltham, Massachusetts, USA

^bmRNA Center of Excellence, Sanofi, Waltham, Massachusetts, USA

^cMyeloid Therapeutics, Cambridge, Massachusetts, USA

ABSTRACT IRES mediated translation initiation requires a different repertoire of factors than canonical cap-dependent translation. Treatments that inhibit the canonical translation factor EIF4G1 have little or no effect on the ability of the *Insr* and *Igf1r* cellular IRESes to promote translation. Transcripts for two cellular receptors contain RNA elements that facilitate translation initiation without intact EIF4G1. Cellular IRES mechanisms may resemble viral type III IRESes allowing them to promote translate with a limited number of initiation factors allowing them to work under stress conditions when canonical translation is repressed.

KEYWORDS insulin receptor, IRES, EIF4G, translational control, internal ribosome entry site, dTAG

INTRODUCTION

Eukaryotic mRNA translation initiation requires a number of factors in order to facilitate recruitment of the ribosome to the 5' end of the mRNA. The 5' 7-methyl guanine (m^7G) cap is bound by the cap binding complex, eukaryotic initiation factor (eIF) 4F, which is composed of three subunits: EIF4E, EIF4A, and EIF4G.¹ The nomenclature surrounding the names of these genes is complicated so we will use the HUGO Gene Nomenclature Committee (HGNC) approved names when discussing single genes or gene products. For complexes of more than one protein we will use the traditional eIF designation. EIF4E is the cap binding protein which directly binds to the m^7G cap and recruits the other members of the eIF4F complex through its interaction with EIF4G.¹ Because EIF4E is the lowest abundance subunit in the eIF4F complex, cap binding is thought to be the rate limiting step of canonical cap-dependent translation.^{2,3} EIF4A is a member of the DEAD-box family of helicases and uses ATP to unwind secondary structure in the 5' untranslated region (5' UTR) of the mRNA in order to facilitate ribosome binding.^{4,5}

The canonical eIF4F complex is held together by the scaffolding protein EIF4G1 which contains binding sites for the other members of the eIF4F complex. Mammalian cells encode three different paralogues of EIF4G. EIF4G1 is an essential gene and is the canonical member of the eIF4F complex.⁶ EIF4G3 can also assemble into the eIF4F complex but is not essential and is associated with spermatogenesis.⁶ EIF4G2 lacks the EIF4E binding domain and thus cannot form the eIF4F complex but it is essential and has been implicated in alternative forms of both cap-dependent and cap-independent translation initiation.^{7–9} All three paralogues facilitate recruitment of the small subunit of the ribosome through a direct interaction with eIF3.^{10–12} The eIF3 complex contains 13 subunits and together with the eIF2-Met-tRNA^{Met}-GTP ternary complex and the 40S ribosomal subunit make up the 43S pre-initiation complex.^{13–15} Artificially recruiting

© 2023 Taylor & Francis Group, LLC

Address correspondence to Michael T. Marr II, mmarr@brandeis.edu.

Received 22 July 2022

Revised 25 July 2023

Accepted 25 August 2023

the core domain of EIF4G1 to an mRNA is sufficient for recruitment of the ribosome and translation initiation highlighting the central role of this protein in initiation.¹⁶

Internal ribosome entry sites (IRESes) were originally discovered in viruses as an alternative translation initiation mechanism.^{17,18} IRES elements allow for translation initiation independent of the mRNA m⁷G cap which is required for canonical cap-dependent translation. This allows transcripts containing IRES elements to be translated under conditions where canonical translation is repressed by inhibitors such as EIF4E binding protein (EIF4EBP1).¹⁹ The IRES itself is a cis-acting RNA element where activity is generally mediated by RNA secondary structure.^{20,21} This RNA structure allows the UTR of the mRNA to bind directly to components of the translation initiation machinery and recruit them independently of m⁷G cap binding by EIF4E.

Recently, viral IRESes have been categorized into eight classes depending on the minimal initiation factors required to successfully initiate translation.²² IRESes in the *Dicistroviridae* family of viruses, exemplified by cricket paralysis virus (CrPV), are the simplest. They require no translation initiation factors as they are able to directly bind to the A site of the 40S ribosomal to initiate translation. IRESes in the *Flaviviridae* family of viruses, the most well-studied of which is hepatitis C virus (HCV) require eIF3 and a ternary complex, such as eIF2-Met-tRNA_i^{Met}-GTP in order to initiate translation. The largest class of identified viral IRESes are contained within the picornavirus family of viruses. These IRESes not only have the highest requirement for initiation factors but also make use of other IRES trans-acting factors (ITAFs).

While the factor requirements and mechanisms that viral IRES elements employ to engage the ribosome have been well studied, IRES elements in cellular mRNAs are much more poorly understood and do not seem to be as easily classified as their viral counterparts.^{22,23} This may in part be due to the situational nature of cellular IRES activity. Unlike some viral IRESes these cellular transcripts contain an ubiquitous m⁷G cap and, consequently, they can potentially be translated in a canonical cap-dependent manner. The IRES activity becomes important under conditions when the canonical pathway is inhibited such as cellular stress. Many identified cellular IRESes are found in transcripts that encode proteins important under these cellular conditions.

We previously identified cellular IRES elements in transcripts encoding proteins critical for the insulin response in both *Drosophila* and mammalian cells.^{24–26} The insulin receptor (Insr) and insulin-like growth factor receptor (Igf1r) transcripts of *Mus musculus* contain IRES elements that are capable of supporting cap-independent translation.²⁴ This was shown both in vitro using excess m⁷G cap analog to inhibit the cap-binding protein, and in cells using bicistronic reporter constructs where second open reading frame (ORF) translation is dependent on IRES activity. We have also previously shown that these cellular IRESes are resistant to inhibition of the EIF4A helicase by the small molecule inhibitor hippuristanol.^{24,27}

Here we show that translation driven by the Insr and Igf1r 5'UTRs is highly resistant to inhibition or depletion of the canonical translation factor EIF4G1. Taken together these results indicate a noncanonical translation initiation mechanism of the Insr and Igf1r transcripts and support the idea that these transcripts utilize internal ribosome entry for translation initiation. The EIF4G1 scaffold is required for both canonical cap-dependent translation as well as translation driven by several classes of picornavirus IRESes. The findings described here suggest that the factor requirements for translation initiation driven by the Insr and Igf1r 5'UTRs may more closely resemble those of class III viral IRESes or may represent a distinct mechanism altogether.^{22,23} Further work on these important transcripts is necessary to resolve this question.

RESULTS

Insr and Igf1r cellular IRES-mediated translation is stimulated by EIF4G1 cleavage with poliovirus 2A-protease. To begin to examine the EIF4G1 requirement of these two cellular IRESes we started by using 2A-protease, a natural EIF4G1 targeting system from poliovirus. Recombinant poliovirus 2A-protease specifically cleaves EIF4G1,

separating the N-terminal domains containing the EIF4E and PABP binding sites from the C-terminal domain, which binds to RNA, EIF4A and eIF3 (Fig. 1A).²⁸ We expressed the poliovirus 2A-protease as a 6-histidine fusion protein in *Escherichia coli*. The 2A protease fusion protein was partially purified using metal affinity chromatography (Fig. 1C).

Partially purified 2A protease was used to treat rabbit reticulocyte lysate (RRL) translation extracts to cleave the EIF4G1 present in the extract. We assayed the extent of EIF4G1 cleavage by immunoblotting with a monoclonal antibody (clone 2A9 Sigma) raised against amino acids 1500-1599 of EIF4G1 capable of detecting the ~100 kD carboxy-terminal fragment of the cleaved EIF4G1. Using this assay, we determined the optimum amount of 2A required for maximum EIF4G1 cleavage. With the optimized conditions, almost all the detectable EIF4G1 is cleaved (Fig. 1D).

We then programmed the 2A-protease-treated RRL or mock-treated RRL translation extracts with in vitro transcribed, capped and polyadenylated firefly luciferase monocistronic mRNA reporters (Fig. 1B).²⁴ mRNAs containing the 5' untranslated region (UTR) of mouse Insr, mouse Igf1r, hepatitis C virus, or a cap-dependent control reporter were assayed. Translation activity was measured by assaying the firefly luciferase

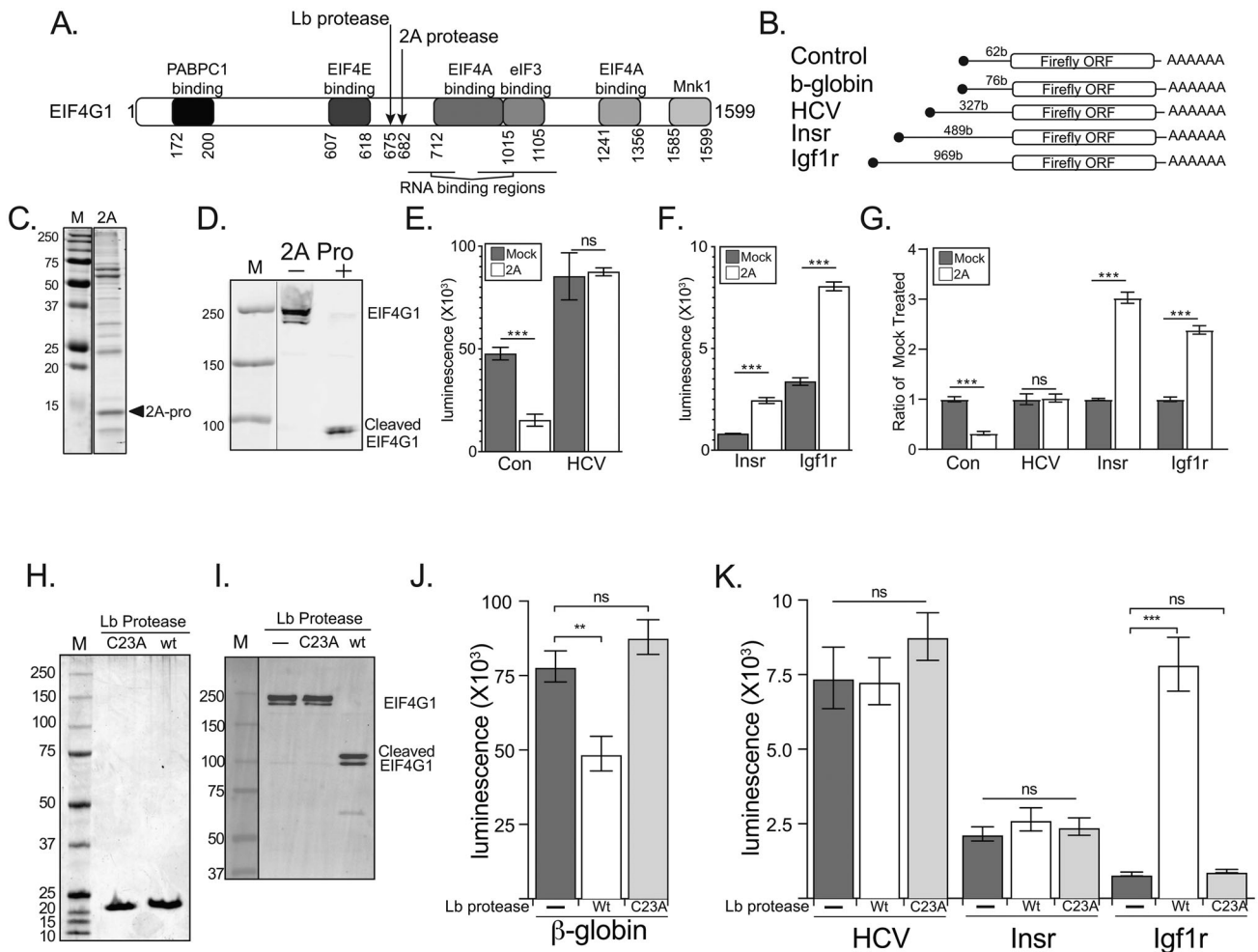


FIG 1 Insr and Igf1r cellular IRESes are resistant to EIF4G1 cleavage by poliovirus 2A-protease in vitro. (A) Schematic of binding domains on EIF4G1. The 2A-protease cleavage site is marked with an arrow. (B) Diagram of RNA reporters used in the in vitro translation assays. (C) SDS-PAGE of partially purified recombinant 2A-protease from *E. coli* imaged by fluorescent imaging of Coomassie stained proteins. (D) Immunoblot showing purified 2A-protease is able to cleave EIF4G1 in RRL translation extracts. (E and F) Activity of the RNA reporters in RRL in vitro translation extracts treated with poliovirus 2A-protease. (G) Reporter activity plotted as the fraction of the respective buffer treated control. (H) SDS-PAGE of recombinant FMDV Lb-protease purified from *E. coli* imaged by fluorescent imaging of Coomassie stained proteins. (I) Immunoblot showing purified FMDV Lb-protease is able to cleave EIF4G1 in RRL translation extracts. (J and K) Activity of the RNA reporters in RRL in vitro translation extracts treated with poliovirus FMDV Lb-protease. (Error bars indicate SEM, * $P < 0.05$, ** $P < 0.01$, *** $P < 0.001$).

produced in 30 min at 37 °C. In the 2A-protease-treated extracts cap-dependent translation is strongly inhibited (Fig. 1E, G). The HCV viral IRES reporter is unaffected by 2A-protease-treatment, indicating that the extract is not generally inhibited and that the deficiency is specifically in cap-dependent translation (Fig. 1E, G). Translation of the RNAs containing the Insr and Igf1r UTRs is not inhibited by EIF4G1 cleavage. In fact, the translation activity of RNAs containing the Insr and Igf1r UTRs is stimulated compared to those of mock-treated extracts (Fig. 1F, G). This result is consistent with previous experiments from our lab and others that have shown Insr and Igf1r IRES containing reporters, as well as those containing HCV or EMCV viral IRESes, have a competitive advantage in nonmicrococcal nuclease treated extracts when cap-dependent translation is inhibited.^{24,29}

Insr and Igf1r cellular IRES-mediated translation is resistant to EIF4G1 cleavage by foot-and-mouth disease virus Lb protease. To corroborate the results with the poliovirus 2A protein we used a second viral protease that targets EIF4G1. The leader protease (Lb) from foot and mouth disease virus (FMDV) also cleaves EIF4G1 at a site close to the 2A cleavage site (Fig. 1A).³⁰ We expressed and purified Lb protease, and a catalytically dead mutant (C23A)³¹ of the Lb protease from *E. coli* (Fig. 1H). The proteins were used to treat RRL translation extracts to cleave the EIF4G1 present in the extract. We assayed the extent of EIF4G1 cleavage by immunoblotting with monoclonal antibody 2A9 as we had for 2A protease. Consistent with previous work, the recombinant Lb protease was capable of cleaving EIF4G1 while Lb-C23A mutant protein had no effect on EIF4G1 (Fig. 1I). We then programmed the Lb-protease-treated RRL or Lb-C23A-treated RRL translation extracts with the in vitro transcribed, capped and polyadenylated firefly luciferase monocistronic mRNA reporters (Fig. 1B). There is no effect of Lb-C23A-treated RRL translation extracts for any of the RNAs tested. However, in the Lb-protease-treated extracts cap-dependent translation is inhibited (Fig. 1J) while the HCV viral IRES reporter is unaffected indicating that the extract is not generally inhibited but that the deficiency is specifically in cap-dependent translation (Fig. 1K). Translation of the RNAs containing the cellular IRESes is uninhibited by the Lb protease treatment despite the complete cleavage of EIF4G1 (Fig. 1K). The Igf1r 5' UTR reporter is actually stimulated by the Lb protease treatment as was seen for the 2A protease treatment (Fig. 1K).

Insr and Igf1r cellular IRES mediated translation is resistant to competitive inhibition by the EIF4G1-eIF3 binding domain. The 2A and Lb protease cleavage of EIF4G1 separates the EIF4E binding region from the eIF3 binding region. However, as seen with the poliovirus IRES, the carboxy terminus of EIF4G1 can function to recruit eIF3 and the 40S subunit by interacting directly with the IRES. To investigate this mechanism for these cellular IRESes, we purified a fragment of EIF4G1 (amino acids 1015–1118) which contains the eIF3 binding site and used it as a competitive inhibitor (Fig. 2A). Previous work has shown that the EIF4G1/eIF3 interaction is mediated by a ~93 amino acid region of EIF4G1.^{10,11,32} Importantly, this binding domain alone can compete with full length EIF4G1 for eIF3 binding and functionally disrupt this interaction.¹²

RRL translation extracts were supplemented with an excess of purified EIF4G1^(1015–1118) and again programmed with the firefly luciferase monocistronic mRNA reporters. The cap-dependent mRNA reporter is inhibited approximately 50% by excess EIF4G1^(1015–1118). We can conclude that the fragment is not generally detrimental to the extract as the HCV viral IRES, which does not require EIF4G1, is unaffected by the excess EIF4G1 fragment (Fig. 2B). In these same conditions the Insr and Igf1r cellular IRESes were also uninhibited (Fig. 2C). In fact, there is a significant, although small, stimulation of the translation activity for the cellular IRES containing transcripts (Fig. 2D).

The Insr and Igf1r cellular IRESes are resistant to inhibition by the EIF4G1^(1015–1118) fragment in mammalian cells. In order to test the EIF4G1 requirements for the Insr and Igf1r IRESes in a cellular context we employed our well characterized bicistronic reporter constructs that we have previously used to test EIF4E and

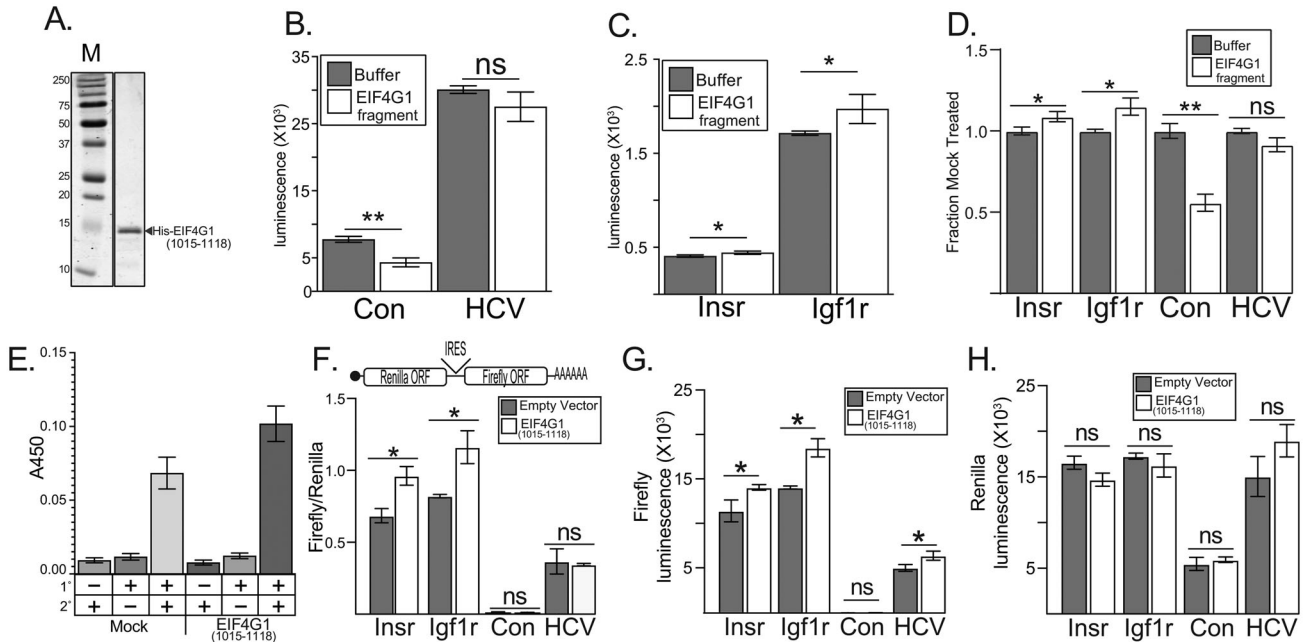


FIG 2 Insr and Igf1r cellular IRESes are resistant to competitive inhibition of EIF4G1/eIF3 interaction by EIF4G1⁽¹⁰¹⁵⁻¹¹¹⁸⁾ fragment. (A) SDS-PAGE of recombinant EIF4G1⁽¹⁰¹⁵⁻¹¹¹⁸⁾ fragment purified from *E. coli*. (B) Luciferase activity of control and HCV RNA reporters in RRL in vitro translation extracts (37°C 30 min) with and without 130 nM EIF4G1⁽¹⁰¹⁵⁻¹¹¹⁸⁾ fragment. (C) Luciferase activity of Insr and Igf1r RNA reporters in RRL in vitro translation extracts (37°C 30 min) with and without 130 nM EIF4G1⁽¹⁰¹⁵⁻¹¹¹⁸⁾ fragment. (D) Reporter data are plotted as the fraction of the respective buffer treated control. (E) ELISA detection of EIF4G1⁽¹⁰¹⁵⁻¹¹¹⁸⁾ expression in transient transfection assays. (F) IRES activity of transiently transfected bicistronic reporters shown as firefly to Renilla ratio. Reporters were cotransfected with an empty vector control or a vector expressing the EIF4G1⁽¹⁰¹⁵⁻¹¹¹⁸⁾ fragment. (G) Firefly luciferase activity of these reporters. (H) Renilla luciferase activity of these reporters. (Error bars indicate SD, **P* ≤ 0.05, ***P* ≤ 0.01).

EIF4A requirements.²⁴ In these constructs the UTR of interest is cloned between a Renilla luciferase ORF and a firefly luciferase ORF. RNA expression is driven by the Rous sarcoma virus LTR promoter creating a single bicistronic mRNA that contains both open reading frames. A diagram of the mRNA produced is shown in the top of Fig. 2F. Translation of Renilla luciferase is cap-dependent while expression of firefly luciferase depends on IRES activity. These reporters were cotransfected with a construct that uses the CMV promoter to drive expression of EIF4G1⁽¹⁰¹⁵⁻¹¹¹⁸⁾ or an empty vector control. ELISA assays indicate the fragment reaches at least 50% the level of endogenous EIF4G1 (Fig. 2E). Compared to the empty vector, coexpression of EIF4G1⁽¹⁰¹⁵⁻¹¹¹⁸⁾ causes a stimulation of Insr and Igf1r IRES activity, measured by the increase in the ratio of firefly luciferase activity to Renilla activity (Fig. 2F). Under these conditions, expression of EIF4G1⁽¹⁰¹⁵⁻¹¹¹⁸⁾ has little effect on Renilla activity itself but the stimulation of IRES activity is evident in the increase of firefly reporter activity alone (Fig. 2G and H).

The Insr and Igf1r cellular IRESes promote translation initiation in the absence of EIF4G1 mammalian cells. To determine the absolute requirement for EIF4G1 in translation initiation mediated by the Insr and Igf1r IRESes we sought to rapidly remove EIF4G1 from the cell. We chose to use targeted degradation based on the dTAG system.^{29,33} This system utilizes FKBP12^{F36V} fusion proteins and a heterobifunctional small molecule to specifically degrade target proteins. A synthetic FKBP12^{F36V} ligand (AP1867) is connected to a small molecule that interacts with an E3 ligase, selectively targeting the fusion protein for degradation. We designed a fusion construct based on the dTAG system that would create an in-frame fusion with the C terminus of EIF4G1 (Fig. 3A). Using CRISPR/cas9 we recombined the construct into the genome of HCT116 cells and tested clones for cassette insertion and EIF4G1 degradation in response to the small molecule ligand.

We first tested the dTAG-13 small molecule. This molecule contains AP1867 attached to a ligand that binds the cereblon E3 ligase.³⁴ Cells were treated with 1 μM dTAG-13 and samples were collected over a 24-h time course. The loss of EIF4G1 was

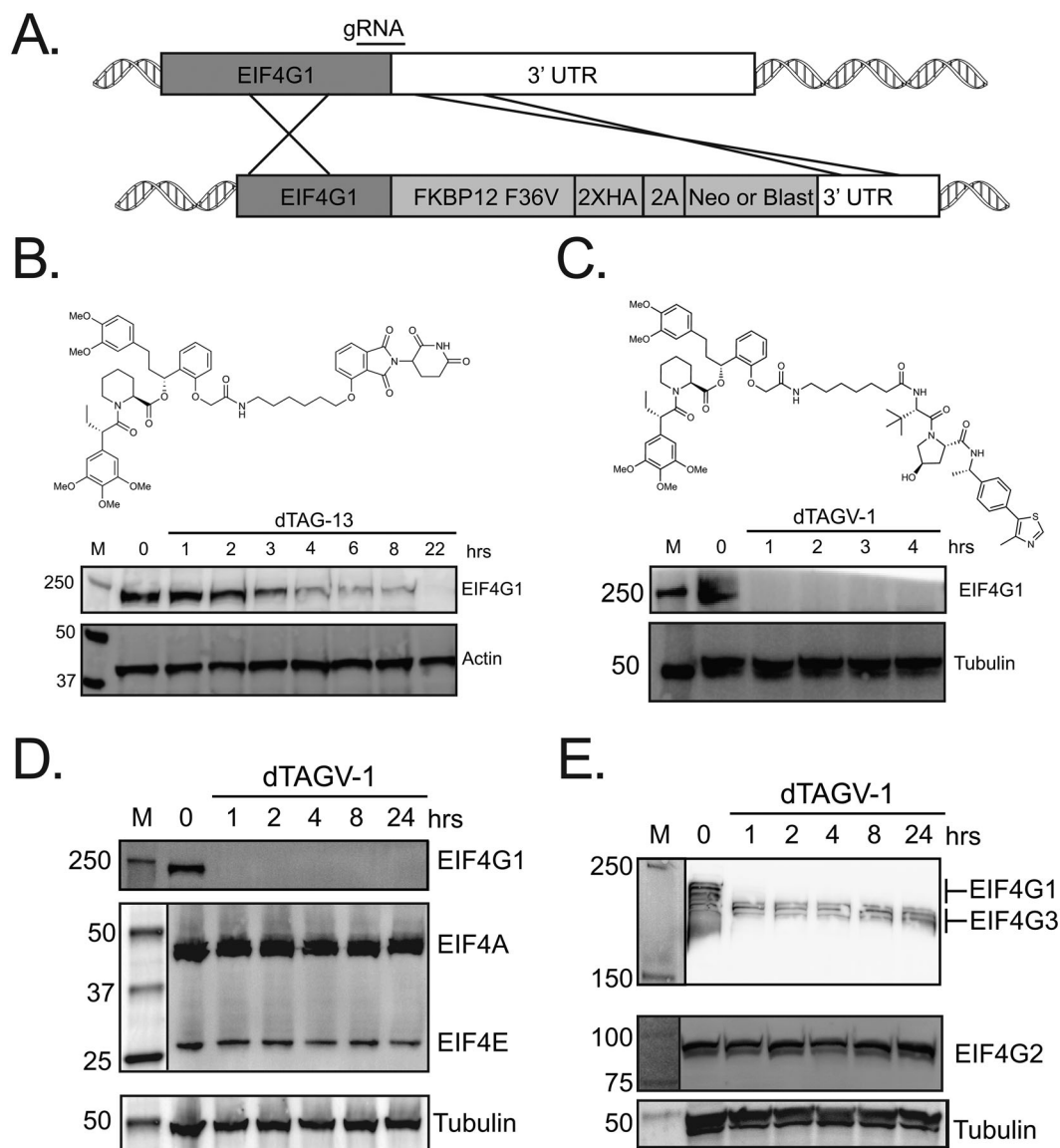


FIG 3 Creation of an EIF4G1 depletion cell line (A) Diagram of the targeting strategy for EIF4G1. (B) Time course of treatment with 1 μ M dTAG-13 small molecule. EIF4G1 is detected by immunoblot, actin detection serves as a loading control. (C) Time course of treatment with 1 μ M dTAGV-1 small molecule. EIF4G1 is detected by immunoblot, tubulin detection serves as a loading control. (D) Time course of treatment with 1 μ M dTAGV-1 small molecule. EIF4G1, EIF4E and EIF4A are detected by immunoblot, tubulin detection serves as a loading control. In the middle panel the molecular weight marker is separated by a line to indicate it was detected in a different fluorescent channel. (E) Immunoblot of EIF4G paralogs. Top panel is probed with antibodies generated against the EIF4G3. EIF4G1 and EIF4G3 bands are indicated. Middle panel is probed with antibodies against EIF4G2. Bottom panel is probed with tubulin antibodies. The molecular weight marker is separated by a line to indicate it was detected in a different fluorescent channel for EIF4G2 and EIF4G3.

assayed by immunoblot. Addition of dTAG-13 was found to cause a significant loss of EIF4G1 from the cell with roughly 50% of the EIF4G1 is depleted in 4 h. However, more than 22 h posttreatment were required to see complete loss of EIF4G1 (Fig. 3B).

Next, we tested the dTAGV-1 small molecule. This molecule is AP1867 attached to a ligand that binds the von Hippel–Lindau (VHL) E3 ligase complex.³³ Cells were treated with 1 μ M dTAGV-1 and time course samples were collected to assay the loss of EIF4G1. Surprisingly, we observed that EIF4G1 is depleted in 1 h (Fig. 3C). Quantitation of the EIF4G1 signal indicates a greater than 99% depletion at that timepoint. The combination of this cell line and dTAGV-1 provides a way to rapidly and specifically remove EIF4G1 from the cell. At the same time, we also monitored the other subunits of eIF4F to determine the dependence on EIF4G1 for their stability. There is no appreciable loss of either EIF4A or EIF4E during 24 h of dTAGV-1 treatment in these cells (Fig. 3D).

To determine if there were compensatory changes in the expression of other members of the EIF4G family we performed immunoblots probing EIF4G2 and EIF4G3. To investigate levels of EIF4G3 we utilized a commercial rabbit polyclonal antibody (PA5-31101, Invitrogen) raised against the first 203 amino acids of human EIF4G3. Unfortunately, there are multiple regions of identical amino acids between EIF4G1 and EIF4G3 in this stretch and this leads to some cross reactivity of the polyclonal antibodies. However, we were able to separate the various isoforms of EIF4G1 and EIF4G3 by extended electrophoresis as has been done previously.³⁵ This approach allowed us to determine that all of the EIF4G1 isoforms are depleted by dTAGV-1 addition and that there is no change in the level of EIF4G3 (Fig. 3E). Likewise, there is no change in the level of EIF4G2 at any of the timepoints tested (Fig. 3E).

The ability to rapidly deplete EIF4G1 allowed us to globally test the dependence of translation on EIF4G1 shortly after its degradation in this cell line. As one hour is sufficient to degrade the vast majority of EIF4G1, this rapid, specific degradation minimizes the possibility of confounding cellular compensation. We first looked at global translation using the puromycin incorporation assay. Cells were treated with dTAGV-1 for either 1.5 or 3 h to deplete EIF4G1 (Fig. 4A). This should allow enough time for previously engaged ribosomes to run off their mRNA templates.³⁶ Cells were then pulse labeled with puromycin to detect proteins that are being actively translated. Total cellular protein was separated by SDS PAGE and puromycin incorporation was detected using a monoclonal antibody against puromycin.³⁷ Mock treated cells showed a robust incorporation of puromycin that depended on active translation as evidenced by its complete inhibition by cycloheximide (Fig. 4B). Upon EIF4G1 depletion puromycin incorporation is greatly decreased at 1.5 and 3 h (67% and 80%, respectively) indicating a general but incomplete inhibition of translation (Fig 4B). There clearly remains detectable translation activity in EIF4G1 depleted cells.

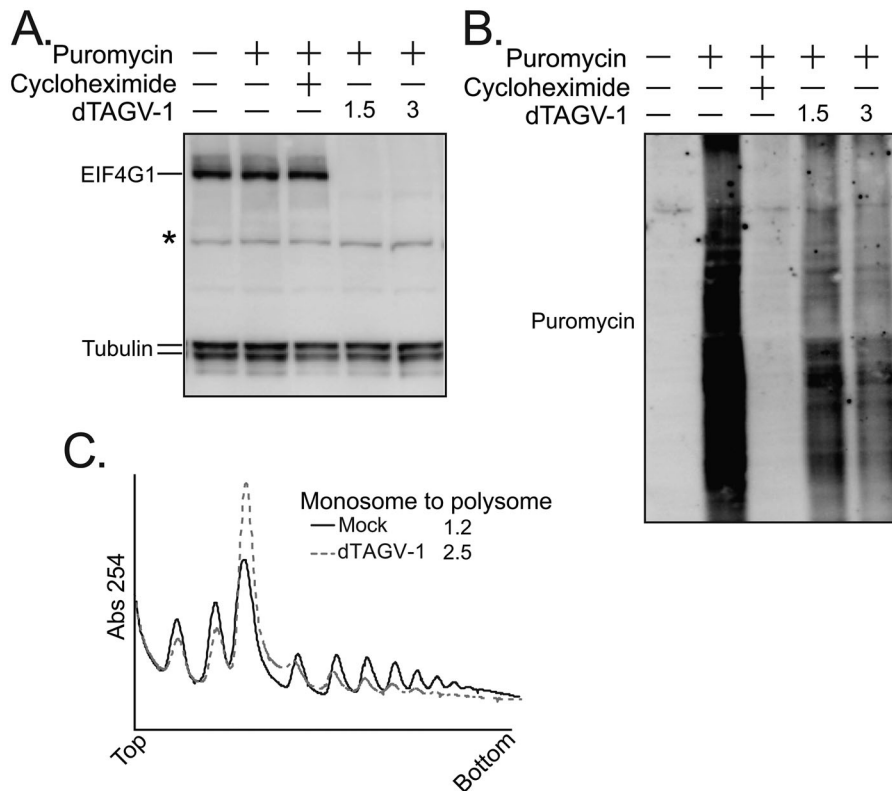


FIG 4 Global effects of EIF4G1 depletion (A) EIF4G1 is detected by immunoblot under the conditions tested for puromycin incorporation, tubulin detection serves as a loading control. (B) The same membrane as in A but blotted with antipuromycin antibodies and detected in a separate channel. (C) Polysome profile of EIF4G1 dTAG line treated with dTAGV-1 for 1.5 h.

To investigate the effect of EIF4G1 depletion on polysomes, cytoplasmic extracts were separated on a sucrose gradient and ribosomes were monitored by absorbance at 254 nm. Comparison of mock treated cells with cells that have been treated with dTAGV-1 indicates a preferential loss of heavy polysomes. There is a concomitant increase in the population of monosomes in EIF4G1 depleted cells leading to a drastic increase in the monosome to polysome ratio (Fig. 4C).

We tested the activity of the Insr, Igf1r and HCV IRES in the EIF4G1 dTAG cell line using the bicistronic system described above. Cells were treated with dTAGV-1 for 1.5 h to deplete endogenous EIF4G1. Mock treated cells were given an equivalent volume of the solvent used to dissolve the dTAGV-1 (DMSO). Under these conditions the cap-dependent Renilla signal is reduced 30–50% (Fig. 5A) for all reporters. Surprisingly, the HCV IRES dependent firefly signal is affected under these conditions, it is reduced to 55% of that of mock cells. In contrast, both the Insr and Igf1r IRES dependent firefly signals retain >75% activity in these conditions (Fig. 5A).

To ensure this result is not a consequence of the bicistronic reporter system we repeated these experiments with monocistronic constructs (Fig. 5B). All IRES constructs

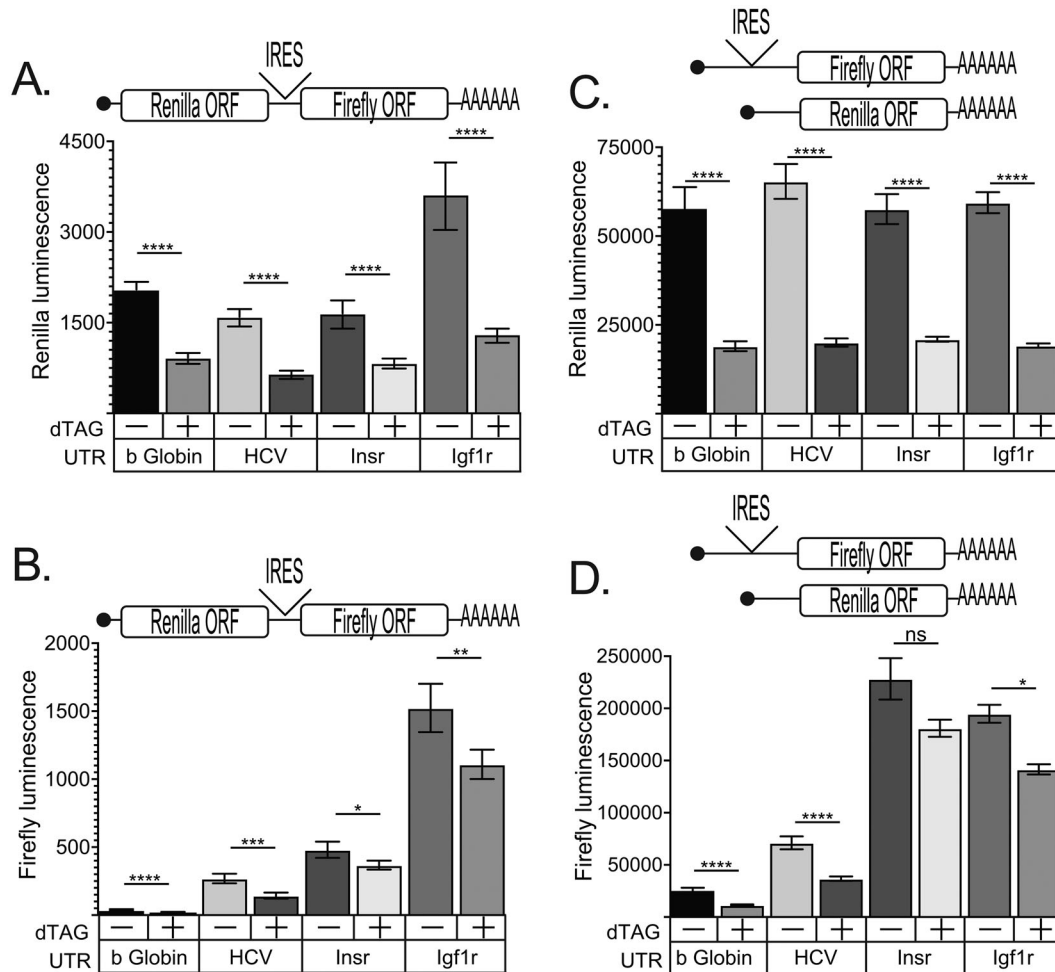


FIG 5 Effects of EIF4G1 depletion on cellular IRESes (A) Renilla luminescence of bicistronic reporters. The first row below the histograms shows the small molecule treatment. dTAG treatment is indicated by a “+” sign. Mock treatment is indicated by “-” sign. The second row indicates the insert being assayed. (B) firefly luminescence of bicistronic reporters. The first row below the histograms shows small molecule treatment. dTAG treatment is indicated by a “+” sign. Mock treatment is indicated by “-” sign. The second row indicates the insert being assayed. (C) Renilla luminescence of monocistronic reporters. The first row below the histograms shows small molecule treatment. dTAG treatment is indicated by a “+” sign. Mock treatment is indicated by “-” sign. The second row indicates the insert being assayed. The histogram reflects the average of four biological replicates each assayed in triplicate. (D) Firefly luminescence of monocistronic reporters. The first row below the histograms shows small molecule treatment. dTAG treatment is indicated by a “+” sign. Mock treatment is indicated by “-” sign. The second row indicates the insert being assayed. The histogram reflects the average of three biological replicates each assayed in triplicate. (Error bars indicate SEM, * $P \leq 0.05$, ** $P \leq 0.01$, *** $P \leq 0.001$, **** $P \leq 0.0001$).

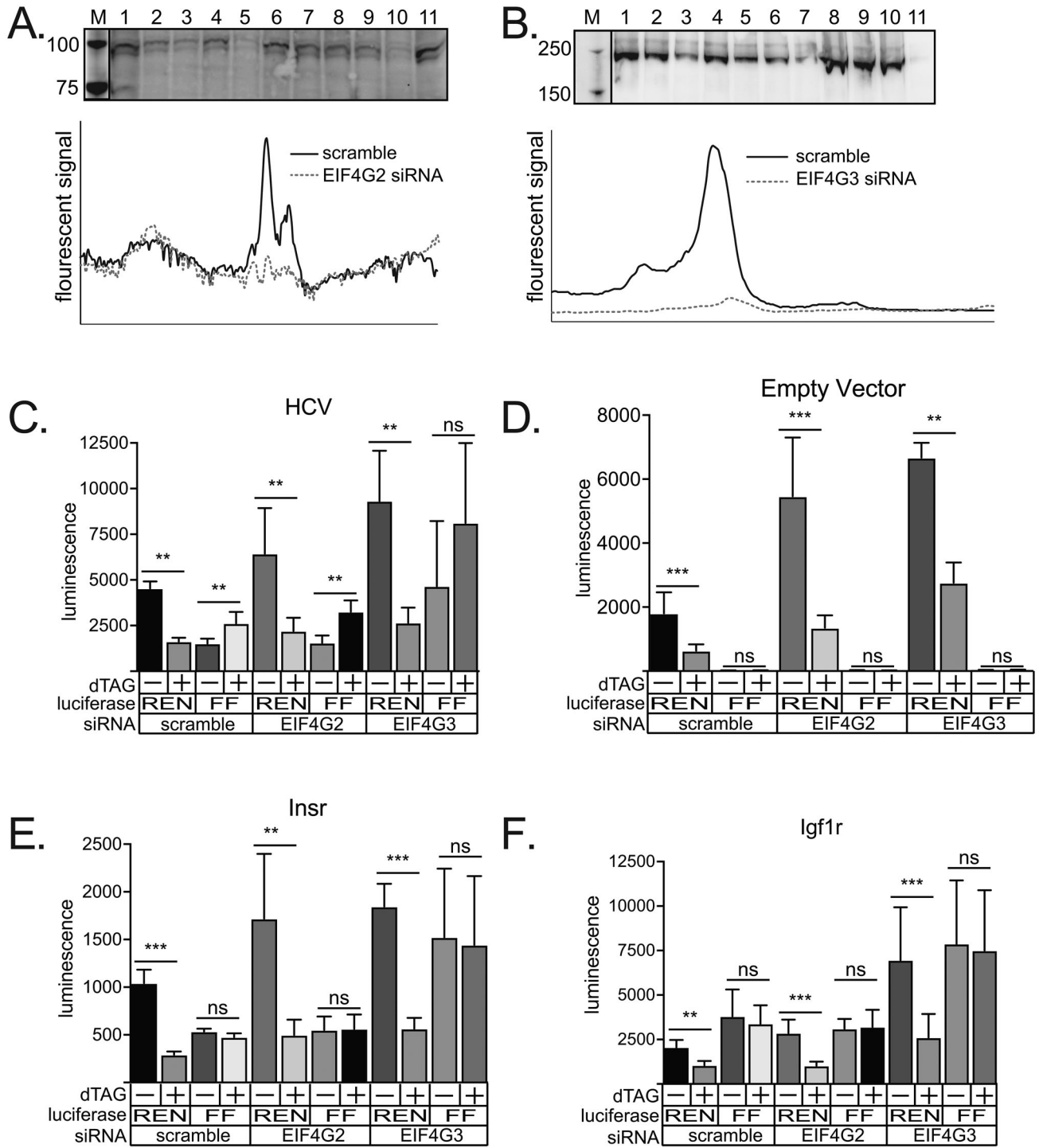


FIG 6 Effects of EIF4G2 and EIF4G3 depletion on cellular IRESes (A) (Top) Immunoblot of EIF4G2 siRNA treatment. M indicates molecular weight markers imaged in a different channel. lane1 scramble (48 h), lane 2. siRNA #1 10 nM (48 h), lane 3. siRNA #2 10 nM (48 h), lane 4. siRNA #3 10 nM (48 h), lane 5. Pool 10 nM Each (48 h), lane 6. scramble (72 h), lane 7. siRNA #1 10 nM (72 h), lane 8. siRNA #2 10 nM (72 h), lane 9. siRNA #3 10 nM (72 h), lane 10. Pool 10 nM Each (72 h), lane 11. scramble (72 h). (Bottom) Lane trace of matched scramble (lane 11) versus optimal siRNA treatment (lane 10). (B) (Top) Immunoblot of EIF4G3 siRNA. M indicates molecular weight markers imaged in a different channel. Lane 1 scramble (48 h), Lane 2. scramble (48 h), Lane 3. siRNA #1 20 nM (48 h), Lane 4. siRNA #2 20 nM (48 h), Lane 5. siRNA #3 20 nM (48 h), Lane 6. Pool 20 nM Each (48 h), Lane 7. Pool 20 nM Each (72 h), Lane 8. siRNA #1 30 nM (72 h), Lane 9. siRNA #2 30 nM (72 h), Lane 10. siRNA #3 30 nM (72 h), Lane 11. Pool 30 nM Each (72 h); (bottom) Plot profile of matched scramble (lane 2) vs optimal siRNA treatment (lane 11) (C-F). Luminescence readings for the inducible bicistronic IRES reporters or empty vector. The individual reporters being assayed are indicated above the histogram. The first row below the histograms shows small molecule treatment. dTAG treatment is indicated by a “+” sign. Mock treatment is indicated by “-” sign. The second row indicates the luciferase being assayed. REN indicates Renilla luciferase signal. FF indicates firefly signal. The target of the siRNAs used are indicated in the bottom row. The histogram reflects the average of four biological replicates each assayed in triplicate. (Error bars indicate SEM, * $P \leq 0.05$, ** $P \leq 0.01$, *** $P \leq 0.001$, **** $P \leq 0.0001$).

were cotransfected with the same cap-dependent monocistronic Renilla reporter plasmid. We found that the effect of EIF4G1 depletion on the monocistronic Renilla construct to be more inhibitory as the cap-dependent translation reporter dropped to 30% when EIF4G1 was depleted in all transfections (Fig. 5B). Again, the HCV IRES retains greater than 50% activity in these depletion conditions and consistent with the bicistronic assay, the Insr and Igf1r cellular IRESes retain greater than 75% activity indicating a robust resilience to the depletion of EIF4G1 (Fig. 5B).

To address the possibility of compensation by other members of the EIF4G family we used Dicer-Substrate Short Interfering RNAs (DsiRNAs)³⁸ to deplete EIF4G2 or EIF4G3 in conditions of EIF4G1 degradation. First, we identified DsiRNA conditions that lead to significant depletion of either EIF4G2 or EIF4G3. The optimum depletion of EIF4G2 was achieved using a mixture of three different DsiRNAs and a concentration of 10 nM each (Fig. 6A, lane 10). The optimum depletion of EIF4G3 was achieved using a mixture of three different DsiRNAs and a concentration of 30 nM each (Fig. 6B, lane 11).

To assay the effects of the depletions we utilized a doxycycline inducible bicistronic reporter. Cells were transfected with a plasmid containing a tetracycline inducible promoter driving expression of a bicistronic mRNA. Renilla luciferase is the first open reading frame and is cap-dependent. Firefly luciferase is the second open reading frame and requires internal entry of the ribosome for translation. Using an inducible reporter allowed for the start of depletion and degradation of targets before inducing the reporter mRNAs. In this paradigm, degradation of EIF4G1 caused a marked decrease in the expression of the cap-dependent Renilla ORF for the constructs tested (Fig. 6C-F). In contrast, depletion of EIF4G1 had no effect on IRES driven reporter expression for the Insr and Igf1r cellular IRES reporters (Fig. 6E and F). For the HCV IRES, depletion of EIF4G1 causes an increase in expression of the second ORF (Fig. 6C). In all conditions the empty vector showed no firefly luciferase activity above background (Fig. 6D).

To assess the possibility of compensation we combined EIF4G1 degradation with DsiRNA depletion of EIF4G2 or EIF4G3. In the absence of EIF4G1 degradation, neither EIF4G2 nor EIF4G3 depletion had any significant effect on reporter expression. Similarly, in combination with EIF4G1 degradation, neither EIF4G2 nor EIF4G3 depletion had any significant effect on the change seen in cap-dependent Renilla luciferase levels. Finally, in combination with EIF4G1 degradation, neither EIF4G2 nor EIF4G3 depletion had any significant effect on IRES mediated firefly luciferase reporter expression (Fig. 6C, E and F).

DISCUSSION

While the mechanisms of many viral IRESes are very well characterized,²² cellular IRES elements are much more poorly understood. Our lab has previously shown that the Insr and Igf1r transcripts contain IRES elements in their 5' UTRs that are able to support translation initiation cap-independently *in vitro* and are able facilitate internal initiation on bicistronic reporter constructs *in vitro* and in cells. It has also been shown that these IRES are able to function independently of the initiation factor EIF4A.²⁴ However, the precise mechanisms by which these cellular IRES elements function are still not understood.

The translation factor EIF4G1 is critical for canonical cap-dependent translation and is also utilized by a number of viral IRESes for noncanonical initiation.^{17,39} In addition, recruitment of EIF4G1 to an mRNA is sufficient to recruit the ribosome and initiate translation through its interaction with eIF3.¹⁶ In order to test the requirement for EIF4G1 in translation initiation driven by the Insr and Igf1r cellular IRESes *in vitro* we perturbed EIF4G1 in two ways.

First, we utilized recombinant viral proteases that specifically cleave EIF4G1 separating N-terminal EIF4E and PABP binding domains from the C-terminal EIF4A and eIF3 binding domains. Using RRL *in vitro* translation assays we show that Insr and Igf1r reporter constructs are unaffected or stimulated by the cleavage of EIF4G1, a result similar to one previously reported using *in vitro* cap competition experiments.²⁴ We

suspect that the stimulation represents an increased availability of translational machinery to the Insr and Igf1r reporters, as translation machinery has been re-tasked from mRNAs endogenous to the RRL extracts whose translation initiation is EIF4G1 dependent.²⁹ This result is consistent with the idea that the mRNAs containing the Insr and Igf1r UTRs support translation initiation under conditions of a compromised EIF4G1.

Second, we used a recombinant EIF4G1 fragment to competitively inhibit the EIF4G1/eIF3 interaction that is thought to lead to ribosome recruitment. When EIF4G1^(1015–1118) is added to *in vitro* translation extracts cap-dependent translation is specifically inhibited while the Insr and Igf1r IRES remain uninhibited. When this same fragment is expressed in mammalian cells along with bicistronic IRES reporter constructs, the activity of both the Insr and Igf1r UTRs is stimulated as measured by the firefly/Renilla signal ratio.

To investigate the EIF4G1 requirement of the Insr and Igf1r UTRs in cells, we created a cell line derived from the diploid HCT116 colon cancer line that allows the conditional depletion of EIF4G1 using the dTAG system.³⁴ Utilizing the small molecule dTAG-V1 we are able to deplete EIF4G1 from the cell in 1 h. Despite the depletion of the eIF4F scaffold, the levels of the other eIF4F components (EIF4E and EIF4A) are unchanged. Likewise, we find the levels of the other EIF4G family members, EIF4G2 and EIF4G3, are unchanged. EIF4G1 depletion results in an 80% decrease in active translation three hours after addition of the small molecule as measured by puromycin incorporation. Polysome profiles of the depleted cells show a preferential loss of heavy polysomes and an increase in monosomes consistent with an inhibition of translation initiation. The effects of EIF4G1 depletion on global translation, in this cellular context, are much more dramatic than previously reported.⁴⁰ The 20% residual translation could be driven by the remaining EIF4G family members, EIF4G2 and EIF4G3. Interestingly, this residual level of translation correlates well with the predicted level of DAP5 target mRNAs.⁹

These cells allowed us to test the effects of EIF4G1 depletion on the reporter mRNAs in a physiologically relevant context. In the EIF4G1 depleted cells the cap-dependent translation reporter signal was only 30–50% of the mock treated cells indicating a requirement for EIF4G. While the IRES containing reporters were also affected in this paradigm indicating a possible secondary effect, the Insr and Igf1r cellular IRES reporters retained more than 75% activity in both a bicistronic and a monocistronic reporter system, performing as well as, or better than, the HCV IRES under these conditions. Taken together these results indicate that the cellular IRESes sustain a robust translation activity even when EIF4G1 is depleted.

Combining degradation of EIF4G1 with DsiRNA mediated depletion of either EIF4G2 or EIF4G3 allowed us to test for functional compensation by other EIF4G family members. We find no difference in IRES activity for the Insr and Igf1r UTRs when depleting individual EIF4G paralogs in addition to EIF4G1 degradation. These results are consistent with the notion that the Insr and Igf1r UTRs provide IRES activity without any EIF4G family requirement.

Taken together these data suggest that the Insr and Igf1r 5' UTRs are cellular IRESes capable of supporting the initiation of translation independently of the canonical translation factor EIF4G1. They do not rule out, however, that these transcripts may be translated via multiple mechanisms, one of which may be EIF4G1 dependent. Thus, when compared to their viral counterparts, the Insr and Igf1r IRESes seem to be more similar to Class III IRESes than Class I or Class II. The HCV IRES typifies this class and requires only eIF3 and a ternary complex in order to initiate translation, but further work on the cellular IRESes will be necessary to determine their precise mechanism.

MATERIALS AND METHODS

Plasmids and cloning. The open reading frame (ORF) for poliovirus 2A-protease was cloned into pMtac, an *E. coli* expression vector, with an N-terminal 6× histidine tag using PCR and standard cloning methods. EIF4G1^(1015–1118) was cloned into the pET28 (Novagen) *E. coli* expression vector with an N-and

C-terminal 6× His tag using PCR and standard cloning methods. Overlapping oligos (Azenta Life Sciences) for the ORF for foot-and-mouth disease virus (FMDV) Lb-protease were codon optimized for *E. coli* expression and amplified by PCR. The resulting ORF was cloned into pET28 with an N-terminal 6× histidine tag using Gibson assembly. The catalytic dead mutant was made by site directed mutagenesis of codon 23 of Lb protease from cysteine (TGT) to alanine (GCT). Plasmid pLacIRARE2, containing low abundance tRNAs and lacI was purified from Rosetta2(DE3) pLacI cells (Novagen). In vitro transcription templates have been described.²⁴ The monocistronic and bicistronic reporters are based on the plasmid pGLRSVRF this plasmid has been described.²⁴ Briefly, this plasmid contains the Rous Sarcoma Virus long terminal repeat (LTR) driving expression of a bicistronic mRNA containing the Renilla luciferase open reading frame (ORF) and the firefly luciferase ORF followed by the SV40 early polyadenylation signal. The 5' UTRs for HCV, Insr, and Igf1r are inserted between the open reading frames. The monocistronic vector was created by removal of the Renilla luciferase ORF by cutting the bicistronic plasmid with restriction enzymes flanking the ORF, blunting the backbone and recircularizing the plasmid by ligation. The inducible bicistronic reporters are based on the plasmid pSBtet-Pur.⁴¹ The various bicistronic reporters were subcloned between the doxycycline inducible promoter and the SV40 polyadenylation signal.

Purification of His-tagged poliovirus 2A-protease, FMDV Lb-protease and EIF4G1⁽¹⁰¹⁵⁻¹¹¹⁸⁾. Expression plasmids were transformed into the BL21*(DE3) *E. coli* strain (Invitrogen) containing the pLacIRARE2 plasmid (Novagen). Cultures were grown to ~0.5 OD₆₀₀ and induced with 1 mM IPTG overnight at 25 °C. EIF4G1⁽¹⁰¹⁵⁻¹¹¹⁸⁾ was purified using Ni Sepharose 6 Fast Flow (GE Healthcare) according to manufacturer's instructions and eluted using 500 mM imidazole. 2A-protease was purified using the same procedure with the addition of 0.1% sarkosyl during protein extraction to solubilize the 2A protein. Both proteins were dialyzed into storage buffer: 50 mM Tris pH7.5 150 mM NaCl 10% glycerol; snap frozen and stored at -80 °C.

FMDV Lb protease and the catalytically dead mutant were purified using magnetic Ni-NTA resin (Thermo Fisher) following manufacturer's recommendations. The eluted proteins were further purified by anion exchange chromatography on Applied Biosystems POROS HQ Strong Anion Exchange Media. The column was equilibrated in 50 mM Tris 8.0, 2 mM DTT, 0.1 mM EDTA, 150 mM NaCl, 5% glycerol. Proteins were eluted with a linear gradient from 150 mM NaCl to 500 mM NaCl in the same buffer. Fractions containing the Lb protein eluted at approximately 200 mM NaCl. Fractions containing Lb proteins were concentrated using Biomax (Millipore) concentrators with a 10 kD cutoff. An equal volume of glycerol was added and the proteins were stored at -20 °C in 25 mM Tris pH8.0, 1 mM DTT, 0.05 mM EDTA, 100 mM NaCl, 50% glycerol.

Immunoblots. For in vitro experiments 6 μL RRL treated with 1 μL purified 2A-protease were loaded onto a 10% SDS-PAGE gel. For cell-based assays 40 μg total protein were used. Separated proteins were transferred to a nitrocellulose membrane. Blots were probed with mouse anti-EIF4G1 monoclonal antibody (clone2A9, Sigma) (1:1000) and imaged using DyLight secondary antibodies (Thermo). For cell-based assays, membranes were probed with the following antibodies: anti-EIF4G rabbit monoclonal antibody (1:5000, C45A4, Cell Signaling), mouse monoclonal anti-HA (clone 12CA5), mouse monoclonal E7 α-tubulin antibody (1:500, Developmental Studies Hybridoma Bank (DSHB)), EIF4E Rabbit monoclonal Ab (1:1000, C46H6, Cell Signaling), EIF4A rabbit monoclonal Ab (1:1000, C32B4, Cell Signaling), β-actin mouse monoclonal Ab (1:1000, 8H10D10, Cell Signaling), EIF4G3 polyclonal rabbit antibody PA5-31101 (1:2000, Invitrogen), DAP5 (EIF4G2) polyclonal rabbit antibody 8HCLC (1 μg/mL, Invitrogen) and detected using DyLight infrared secondary antibodies (Thermo) on a ChemiDocMP imager (Bio-rad).

ELISA-96 well microtiter plate wells were coated with 100 μL of total cell lysate, at a concentration of 1 and 10 μg/mL total protein in carbonate buffer pH9.6 overnight at 4 °C. The wells were washed three times in wash buffer-phosphate buffered saline (PBS) containing 0.05% v/v Tween20. Then 150 μL of blocking solution (PBS containing 1% w/v BSA) was added to each well and incubated for 1 h at 37 °C. The wells were washed four times in wash buffer. One hundred microliters of unconjugated detection antibody SAB4500741 (Sigma) diluted 1:1000 in wash buffer was added to each well and incubated for 1 h at 37 °C. The wells were washed three times in wash buffer. One hundred microliters HRP-conjugated secondary antibody diluted 1:1000 in wash buffer was added to each well and incubated for 1 h at 37 °C. The wells were washed three times in wash buffer. One hundred microliters of TMB Core+ (Bio-Rad) solution was added to each well and incubate at room temperature (for 30 min. Fifty microliters of stop solution (0.2 M H₂SO₄) was added and absorbance values were measured at 450 nm.

In vitro transcription and RNA reporter preparation. Transcription templates for RNA reporters were prepared by digesting plasmid templates containing the UTRs of interest upstream of a firefly luciferase ORF all under the control of a T7 or T3 reporter. Templates were purified using a column DNA clean up protocol (Bio Basic) and eluted in TE pH8.0. Templates were transcribed using T3 or T7 RNA polymerase for 4 h at 37 °C and purified using LiCl precipitation. A 5' 7mG cap was added to the RNA reporters using vaccinia virus capping enzyme (NEB) according to the manufacturer's protocol. Capped reporters were purified using phenol/chloroform extraction and isopropanol precipitation. RNAs were then 3' poly(A) tailed using *E. coli* poly(A) polymerase (NEB) and purified using phenol/chloroform extraction and isopropanol precipitation.

In vitro translation. Translation assays were done in a 10 μL reaction volume using 6 μL of whole rabbit reticulocyte lysate still containing endogenous mRNAs to allow for competitive conditions. Translation extracts were pre-incubated with 130 nM EIF4G1⁽¹⁰¹⁵⁻¹¹¹⁸⁾ for 10 min at 30 °C, 2A-protease for 1.5 h at 30 °C, FMDV Lb or C23A protease (10 ng) 5 min on ice or the respective buffer control. Translation reactions also contained: 24 mM HEPES pH 7.4, 0.4 or 1 mM magnesium acetate, 30 mM potassium acetate, 16.8 mM creatine phosphate, 0.1 mM spermidine, 60 μM amino acids, 800 ng creatine kinase, 1 μg calf liver tRNA, and between 15 and 100 ng of reporter RNA. Translation reactions were

incubated at 37 °C for 30 min for 2A protease and EIF4G fragment experiments and 30 °C for 30 min for FMDV Lb experiments. Luciferase activity was measured using 100 μ L of luciferase reagent: 75 mM HEPES pH8.0, 5 mM MgSO₄, 20 mM DTT, 530 μ M ATP, 100 μ M EDTA, 500 μ M coenzyme A, and 500 μ M D-luciferin.

Cell culture, transient transfections, bicistronic dual luciferase assay. HEK293T and HCT116 cells were maintained in Dulbecco's Modified Eagle's Medium supplemented with 10% FetalPlex (Gemini Bio), 1 \times penicillin/streptomycin, 1 μ g/mL insulin. For transient transfection of HEK293T, cells were seeded in a 24-well plate at a density to be ~60% confluent at the time of transfection and all transfections were performed with a 1:5 bicistronic reporter to expression vector ratio. HEK293T cells were transfected with bicistronic reporter plasmids and either CMV driven EIF4G1⁽¹⁰¹⁵⁻¹¹¹⁸⁾, or an empty FLAG-tag expression vector with polyethylenimine at a 3:1 PEI to DNA ratio. EIF4G1⁽¹⁰¹⁵⁻¹¹¹⁸⁾ experiments were harvested 48 h after transfection with Passive Lysis Buffer (Promega). HCT116 cells were seeded at a density of 8 \times 10⁴ cells per milliliter for a 72 h total incubation period, transfected with jetPRIME (Polyplus) according to manufacturer's protocol and maintained with a subculture ratio of 1:6. CMV driven EIF4G1⁽¹⁰¹⁵⁻¹¹¹⁸⁾ transfections were harvested after 72 h. Firefly and Renilla activity were measured using a dual-luciferase approach. First, firefly luciferase was measured in 75 mM HEPES pH8.0, 5 mM MgSO₄, 20 mM DTT, 530 μ M ATP, 100 μ M EDTA, 500 μ M coenzyme A, and 500 μ M D-luciferin. Then Renilla luciferase was measured by adding an equal volume of 1.0 M NaCl, 500 mM Na₂SO₄, 25 mM Na₄PPI, 15 mM EDTA, 10 mM NaOAc, and 0.1 mM coelenterazine.

Generation of EIF4G1 dTAG line. EIF4G1 targeting constructs were based on plasmid pCRIS-PITChv2-dTAG-BSD (BRD4) a gift from James Bradner & Behnam Nabet (Addgene plasmid # 91795).³⁴ This construct contains the FKBP_F36V-2xHA-P2A-BSD (dTAG) cassette encoding, in frame, the FKBP_F36V protein followed by two copies of the HA epitope, a 2A peptide from porcine teschovirus-1 polyprotein and a blasticidin resistance marker. DNA corresponding to 271 bp upstream of the EIF4G1 stop codon was amplified by PCR from HCT116 genomic DNA and inserted in frame with the dTAG coding sequence. In the PCR process, silent mutations were introduced in the coding region for the last five amino acids of EIF4G to prevent CRISPR/Cas9 from targeting the recombinant locus. Subsequently, DNA corresponding to 449 bp downstream of the stop codon was amplified by PCR from HCT116 genomic DNA and inserted after the dTAG cassette. A second construct containing the neomycin resistance marker in place of the blasticidin resistance marker was created.

A guide RNA expressing plasmid (phU6_EIF4G1_gRNA_2611) was created by inserting annealed, phosphorylated oligonucleotides (caccGAGGAGTCTGACCACAACCTG, aaacCAGTTGTGGTCAGACTCCTC) targeting the last 20 bases of EIF4G1 into the BbsI site of phU6, a derivative of pX330-U6-Chimeric_BB-CBh-hSpCas9 (a gift from Feng Zhang Addgene plasmid # 42230) lacking the Cas9 expression cassette.

The neomycin and blasticidin targeting constructs were cotransfected into HCT116 cells using JetPrime (Polyplus) along with phU6_EIF4G1_gRNA_2611 and pJDS246 expressing cas9. pJDS246 was a gift from Keith Joung (Addgene plasmid # 43861). After three days the cells were treated with 30 μ g/mL blasticidin followed by 100 μ g/mL G418. Cell lines were cloned by picking resistant colonies followed by cloning by dilution. Cell lines were screened for insertion by PCR and by immunoblot. Positive lines were tested for EIF4G1 degradation using 1 μ M dTAG-13 and 1 μ M dTAGV-1.

EIF4G1 degradation. To achieve EIF4G1 degradation in the HCT116 C8 clonal line, 1 μ M dTAGV-1 (Tocris Bioscience) was added in complete media and incubated for 1.5 h at 37 °C before any assays were conducted, including reporter transient transfections, puromycin incorporation, and polysome gradient centrifugation. Mock treated cells receive an equivalent volume of solvent (DMSO) used to dissolve the small molecule.

siRNA experiments. Dicer-Substrate Short Interfering RNAs (DsiRNAs) were purchased from Integrated DNA Technologies as TriFECTa RNAi Kits targeting EIF4G2 (hs.Ri.EIF4G2.13) or EIF4G3 (hs.Ri.EIF4G3.13). Each kit contains three targeting DsiRNAs. For EIF4G2 a pool of 10 nM of all three DsiRNAs was used for targeting. For EIF4G3 a pool of 30 nM of all three DsiRNAs was used for targeting. A scrambled DsiRNA was used as a control.

HCT116 EIF4G1-dTAG C8 cells were seeded in a 24-well plate at a density of 100,000 cells per well. After 24 h cells were transfected with a doxycycline inducible bicistronic reporter plasmid (0.07 μ g per well) and DsiRNA via Polyplus jetPrime transfection system.

Cells were incubated for 24 h and split 1:3. Cell were incubated a further 24 h before treatment with 10 μ g/mL doxycycline. For depletion of EIF4G1, 1 μ M dTagV-1 (or an equivalent volume of solvent) was added. Posttreatment, cells were incubated for 48 h, harvested with 1 \times Passive Lysis buffer (Promega) and frozen overnight at -20 °C. Firefly luciferase and Renilla luciferase were measured as described above.

Polysome gradient centrifugation. Eleven milliliters, 1050% sucrose gradients were prepared in Beckman polyallomer tubes (No. 331372). Gradients were assembled by layering 11 levels of 1 mL sucrose solution with gradually decreasing concentrations, from 1.5 M to 0.5 M. These sucrose solutions were buffered using 50 mM Tris pH7.5, 0.25 M KCl, and 50 mM MgCl₂ and supplemented with 0.1 mg/mL cycloheximide. Each sucrose layer was added with an 1 mL serological pipet (using gravity mode) without disrupting the separating surface. Gradients were sealed with Parafilm, stored at -80 °C and thawed at 4 °C overnight before use. Cells were incubated with 0.1 mg/mL cycloheximide for 5 min at 37 °C. Cells were harvested in media, centrifuged at 800 \times g for 5 min, and washed with 1 mL ice-cold PBS with 0.1 mg/mL cycloheximide. Cells were centrifuged at 15 \times g for 5 min at 4 °C. Cell pellets were flash frozen in liquid nitrogen and stored overnight at -80 °C. Cell pellets were lysed in 20 mM HEPES pH7.4, 150 KCl, 2.5 mM MgOAc₂, 1% Triton X-100, 1X EDTA-free protease inhibitors (Sigma), 1 mM Dithiothreitol (DTT),

0.1 mg/mL cycloheximide, and 0.1 μ L/mL Supersel (Life Technologies) for 10 min on ice and centrifuged at $21,000\times g$ for 10 min at 4 °C. Fifteen A260 units of induced and uninduced extracts were loaded onto 11 mL sucrose gradients described previously. Sucrose gradients were centrifuged for 2 h at 35,000 rpm in a SW41 Ti rotor in a Beckman ultracentrifuge. Gradients were then collected using a Brandel syringe pump and A254 was measured using a Teledyne Isco UA-6 absorbance detector.

Puromycin incorporation assay. Cells were treated with 1 μ M dTAGV-1 as indicated. For cycloheximide treated samples, cells were treated with 0.1 mg/mL cycloheximide for 5 min at 37 °C. All samples were then incubated with 10 μ g/mL puromycin for 30 min at 37 °C. Cells were harvested in 1 \times RIPA buffer (20 mM Tris-HCl (pH 7.5), 150 mM NaCl, 1 mM Na₂EDTA, 1 mM EGTA, 1% NP-40, 1% sodium deoxycholate, 2.5 mM sodium pyrophosphate, 1 mM β -glycerophosphate, 1 mM Na₃VO₄, and 1 μ g/mL leupeptin with 1 \times EDTA-free protease inhibitors (Sigma)). Protein concentrations were determined using BCA assay (Pierce) and equal amounts of protein were loaded onto a 4–12% SDS-PAGE gel. Protein was transferred to an activated (PVDF) membrane, blocked, and probed with either mouse antipuumycin antibody PMY:2A4 (1:1000, (DSHB)) and mouse E7 α -tubulin antibody (1:500, DSHB). The antipuumycin PMY:2A4 antibody has been described.³⁷

ACKNOWLEDGEMENTS

NKC and MTH were supported for a portion of the work by a training grant from the NIH (T32 GM007122). A portion of the work was supported by a grant to MTM (R01GM117034).

AUTHOR CONTRIBUTIONS

MTM and NKC conceived the study and wrote the paper. NK, MTH, ZK, WBD and MTM performed the experiments. MTM, MTH, ZK, WBD and NK analyzed the results and edited and approved the final version of the manuscript.

ORCID

Michael T. Marr, II  <http://orcid.org/0000-0002-7366-7987>

DATA AVAILABILITY STATEMENT

The authors confirm that the data supporting the findings of this study are available within the article [and/or] its [supplementary materials](#). Raw data is deposited at Mendeley Data (doi: 10.17632/sh38yh4sh.1).

DISCLOSURE STATEMENT

The authors declare that they have no conflicts of interest with the contents of this paper. The content is solely the responsibility of the authors and does not necessarily represent the official views of the National Institutes of Health.

REFERENCES

- Pelletier J, Sonenberg N. The organizing principles of eukaryotic ribosome recruitment. *Annu Rev Biochem.* 2019;88:307–335. doi:10.1146/annurev-biochem-013118-111042.
- Hiremath LS, Webb NR, Rhoads RE. Immunological detection of the messenger RNA cap-binding protein. *J Biol Chem.* 1985;260:7843–7849. doi:10.1016/S0021-9258(17)39529-7.
- Duncan R, Milburn SC, Hershey JW. Regulated phosphorylation and low abundance of HeLa cell initiation factor eIF-4F suggest a role in translational control. Heat shock effects on eIF-4F. *J Biol Chem.* 1987;262:380–388. doi:10.1016/S0021-9258(19)75938-9.
- Ray BK, Lawson TG, Kramer JC, Cladaras MH, Grifo JA, Abramson RD, Merrick WC, Thach RE. ATP-dependent unwinding of messenger RNA structure by eukaryotic initiation factors. *J Biol Chem.* 1985;260:7651–7658. doi:10.1016/S0021-9258(17)39658-8.
- Pestova TV, Kolupaeva VG. The roles of individual eukaryotic translation initiation factors in ribosomal scanning and initiation codon selection. *Genes Dev.* 2002;16:2906–2922. doi:10.1101/gad.1020902.
- Sénéchal P, Robert F, Cencic R, Yanagiya A, Chu J, Sonenberg N, Paquet M, Pelletier J. Assessing eukaryotic initiation factor 4F subunit essentiality by CRISPR-induced gene ablation in the mouse. *Cell Mol Life Sci.* 2021;78:6709–6719. doi:10.1007/s00018-021-03940-5.
- Yamanaka S, Zhang XY, Maeda M, Miura K, Wang S, Farese RV, Iwao H, Innerarity TL. Essential role of NAT1/p97/DAP5 in embryonic differentiation and the retinoic acid pathway. *Embo J.* 2000;19:5533–5541. doi:10.1093/emboj/19.20.5533.
- Liberman N, Gandin V, Svitkin YV, David M, Virgili G, Jaramillo M, Holcik M, Nagar B, Kimchi A, Sonenberg N, et al. DAP5 associates with eIF2beta and eIF4A1 to promote Internal Ribosome Entry Site driven translation. *Nucleic Acids Res.* 2015;43:3764–3775. doi:10.1093/nar/gkv205.
- de la Parra C, Ernlund A, Alard A, Ruggles K, Ueberheide B, Schneider RJ. A widespread alternate form of cap-dependent mRNA translation initiation. *Nat Commun.* 2018;9:3068. doi:10.1038/s41467-018-05539-0.
- Villa N, Do A, Hershey JWB, Fraser CS. Human eukaryotic initiation factor 4G (eIF4G) protein binds to eIF3c, -d, and -e to promote mRNA recruitment to the ribosome. *J Biol Chem.* 2013;288:32932–32940. doi:10.1074/jbc.M113.517011.
- LeFebvre AK, Korneeva NL, Trutschl M, Cvek U, Duzan RD, Bradley CA, Hershey JWB, Rhoads RE. Translation initiation factor eIF4G-1 binds to eIF3 through the eIF3e subunit. *J Biol Chem.* 2006;281:22917–22932. doi:10.1074/jbc.M605418200.
- Korneeva NL, Lamphear BJ, Hennigan FL, Rhoads RE. Mutually cooperative binding of eukaryotic translation initiation factor (eIF) 3 and eIF4A to human eIF4G-1. *J Biol Chem.* 2000;275:41369–41376. doi:10.1074/jbc.M007525200.
- Phan L, Schoenfeld LW, Valásek L, Nielsen KH, Hinnebusch AG. A subcomplex of three eIF3 subunits binds eIF1 and eIF5 and stimulates ribosome binding of mRNA and tRNA(i)Met. *Embo J.* 2001;20:2954–2965. doi:10.1093/emboj/20.11.2954.

14. Siridechadilok B, Fraser CS, Hall RJ, Doudna JA, Nogales E. Structural roles for human translation factor eIF3 in initiation of protein synthesis. *Science*. 2005;310:1513–1515. doi:10.1126/science.1118977.
15. Majumdar R, Bandyopadhyay A, Maitra U. Mammalian translation initiation factor eIF1 functions with eIF1A and eIF3 in the formation of a stable 40S preinitiation complex. *J Biol Chem*. 2003;278:6580–6587. doi:10.1074/jbc.M210357200.
16. De Gregorio E, Preiss T, Hentze MW. Translation driven by an eIF4G core domain in vivo. *Embo J*. 1999;18:4865–4874. doi:10.1093/emboj/18.17.4865.
17. Pelletier J, Sonenberg N. Internal initiation of translation of eukaryotic mRNA directed by a sequence derived from poliovirus RNA. *Nature*. 1988;334:320–325. doi:10.1038/334320a0.
18. Sonenberg N, Pelletier J. Poliovirus translation: a paradigm for a novel initiation mechanism. *Bioessays*. 1989;11:128–132. doi:10.1002/bies.950110504.
19. Holcik M, Sonenberg N. Translational control in stress and apoptosis. *Nat Rev Mol Cell Biol*. 2005;6:318–327. doi:10.1038/nrm1618.
20. Balvay L, Soto Rifo R, Ricci EP, Decimo D, Ohlmann T. Structural and functional diversity of viral IRESes. *Biochim Biophys Acta*. 2009;1789:542–557. doi:10.1016/j.bbagr.2009.07.005.
21. Fernandez-Miragall O, Lopez de Quinto S, Martinez-Salas E. Relevance of RNA structure for the activity of picornavirus IRES elements. *Virus Res*. 2009;139:172–182. doi:10.1016/j.virusres.2008.07.009.
22. Kwan T, Thompson SR. Noncanonical translation initiation in eukaryotes. *Cold Spring Harb Perspect Biol*. 2019;11:a032672. doi:10.1101/cshperspect.a032672.
23. Jackson RJ. The current status of vertebrate cellular mRNA IRESs. *Cold Spring Harb Perspect Biol*. 2013;5(2). doi:10.1101/cshperspect.a011569.
24. Olson CM, Donovan MR, Spellberg MJ, Marr MT. The insulin receptor cellular IRES confers resistance to eIF4A inhibition. *Elife*. 2013;2:e00542. doi:10.7554/eLife.00542.
25. Marr MT, D'Alessio JA, Puig O, Tjian R. IRES-mediated functional coupling of transcription and translation amplifies insulin receptor feedback. *Genes Dev*. 2007;21:175–183. doi:10.1101/gad.1506407.
26. Vasudevan D, Clark NK, Sam J, Cotham VC, Ueberheide B, Marr MT, Ryou HD. The GCN2-ATF4 signaling pathway induces 4E-BP to bias translation and boost antimicrobial peptide synthesis in response to bacterial infection. *Cell Rep*. 2017;21:2039–2047. doi:10.1016/j.celrep.2017.10.096.
27. Lindqvist L, Oberer M, Reibarkh M, Cencic R, Bordeleau M-E, Vogt E, Marintchev A, Tanaka J, Fagotto F, Altmann M, et al. Selective pharmacological targeting of a DEAD box RNA helicase. *PLoS One*. 2008;3:e1583. doi:10.1371/journal.pone.0001583.
28. Kowarz E, Loscher D, Marschalek R. Optimized Sleeping Beauty transposons rapidly generate stable transgenic cell lines. *Biotechnol J*. 2015;10:647–653. doi:10.1002/biot.201400821.
29. Nabet B, Roberts JM, Buckley DL, Paulk J, Dastjerdi S, Yang A, Leggett AL, Erb MA, Lawlor MA, Souza A, et al. The dTAG system for immediate and target-specific protein degradation. *Nat Chem Biol*. 2018;14:431–441. doi:10.1038/s41589-018-0021-8.
30. David A, Dolan BP, Hickman HD, Knowlton JJ, Clavarino G, Pierre P, Bennisink JR, Yewdell JW. Nuclear translation visualized by ribosome-bound nascent chain puromycylation. *J Cell Biol*. 2012;197:45–57. doi:10.1083/jcb.201112145.
31. Ventoso I, MacMillan SE, Hershey JW, Carrasco L. Poliovirus 2A proteinase cleaves directly the eIF-4G subunit of eIF-4F complex. *FEBS Lett*. 1998;435:79–83. doi:10.1016/S0014-5793(98)01027-8.
32. Svitkin YV, Herdy B, Costa-Mattioli M, Gingras A-C, Raught B, Sonenberg N. Eukaryotic translation initiation factor 4E availability controls the switch between cap-dependent and internal ribosomal entry site-mediated translation. *Mol Cell Biol*. 2005;25:10556–10565. doi:10.1128/MCB.25.23.10556-10565.2005.
33. Kirchwegger R, Ziegler E, Lamphear BJ, Waters D, Liebig HD, Sommergruber W, Sobrino F, Hohenadl C, Blaas D, Rhoads RE, et al. Foot-and-mouth disease virus leader proteinase: purification of the Lb form and determination of its cleavage site on eIF-4 gamma. *J Virol*. 1994;68:5677–5684. doi:10.1128/JVI.68.9.5677-5684.1994.
34. Piccone ME, Zellner M, Kumosinski TF, Mason PW, Grubman MJ. Identification of the active-site residues of the L proteinase of foot-and-mouth disease virus. *J Virol*. 1995;69:4950–4956. doi:10.1128/JVI.69.8.4950-4956.1995.
35. Hinton TM, Coldwell MJ, Carpenter GA, Morley SJ, Pain VM. Functional analysis of individual binding activities of the scaffold protein eIF4G. *J Biol Chem*. 2007;282:1695–1708. doi:10.1074/jbc.M602780200.
36. Nabet B, Ferguson FM, Seong BKA, Kuljanin M, Leggett AL, Mohardt ML, Robichaud A, Conway AS, Buckley DL, Mancias JD, et al. Rapid and direct control of target protein levels with VHL-recruiting dTAG molecules. *Nat Commun*. 2020;11:4687. doi:10.1038/s41467-020-18377-w.
37. Coldwell MJ, Sack U, Cowan JL, Barrett RM, Vlasak M, Sivakumaran K, Morley SJ. Multiple isoforms of the translation initiation factor eIF4GII are generated via use of alternative promoters, splice sites and a non-canonical initiation codon. *Biochem J*. 2012;448:1–11. doi:10.1042/BJ20111765.
38. Ingolia NT, Lareau LF, Weissman JS. Ribosome profiling of mouse embryonic stem cells reveals the complexity and dynamics of mammalian proteomes. *Cell*. 2011;147:789–802. doi:10.1016/j.cell.2011.10.002.
39. Kim D-H, Behlke MA, Rose SD, Chang M-S, Choi S, Rossi JJ. Synthetic dsRNA Dicer substrates enhance RNAi potency and efficacy. *Nat Biotechnol*. 2005;23:222–226. doi:10.1038/nbt1051.
40. Witherell GW, Wimmer E. Encephalomyocarditis virus internal ribosomal entry site RNA-protein interactions. *J Virol*. 1994;68:3183–3192. doi:10.1128/JVI.68.5.3183-3192.1994.
41. Ramirez-Valle F, et al. eIF4G1 links nutrient sensing by mTOR to cell proliferation and inhibition of autophagy. *J Cell Biol*. 2008;181:293–307.